INTRAOPERATIVE MEASUREMENT OF SHOULDER JOINT CONTACT FORCES DURING REVERSE TOTAL SHOULDER ARTHROPLASTY

By

CHIH-CHIANG CHANG

A THESIS PRESENTED TO THE GRADUATE SCHOOL
OF THE UNIVERSITY OF FLORIDA IN PARTIAL FULFILLMENT
OF THE REQUIREMENTS FOR THE DEGREE OF
MASTER OF SCIENCE

UNIVERSITY OF FLORIDA

2013

To my Professors, Dr. Scott A. Banks and Dr. Masaru Higa, who has been my best support in this research and my graduate study

ACKNOWLEDGMENTS

I am grateful to the many people who have supported me as I worked on this thesis and helped me grow, especially my advisor Dr. Scott Arthur Banks, who got me excited about orthopaedic biomechanics and whose professions on both clinics and engineering inspired me to develop an extreme interest in doing research in orthopaedic engineering. I'm indebted to him for trusting me to work on this project, and guiding and developing my skills. This thesis research work would not have been possible without his mentoring and his guidance and encouragement.

I would like to express my gratitude to Dr. Masaru Higa, at University of Hyogo in Japan for trusting me to work on this project with him. I would not be able to accomplish these tasks in this research without his time and effort on training me. I thank for his mentoring and valuable advices. I'm very lucky to gain research experiences by working with him. I would like then to thank Dr. Thomas Wright for also trusting in my abilities to accomplish the task of running the measurement in operation room. I would like to also thank Aimee Struk for her efforts and helps on every measurement task in the hospital. I also want to thank Dr. Bryan Conrad for his training of use of the MTS machine and providing me all the instruments I needed for the calibration.

I'm grateful to everyone in the Orthopaedic Biomechanics Lab. Especially, I would like to thank David Walker for his helps on the data collecting both in operation room and calibration; and I would also like to thank Ira Hill for giving me valuable advices on programming anytime.

Finally, I would like to express my deepest gratitude to my parents for their encouragement in all my endeavors. I would not have been able to go for my dream without their fully support.

TABLE OF CONTENTS

page

LIST OF TABLES

Table page

LIST OF FIGURES

Abstract of Thesis Presented to the Graduate School
of the University of Florida in Partial Fulfillment of the
Requirements for the Degree of Master of Science

INTRAOPERATIVE MEASUREMENT OF SHOULDER JOINT CONTACT FORCES DURING REVERSE TOTAL SHOULDER ARTHROPLASTY

By

Chih-Chiang Chang

May 2013

Chair: Scott Arthur Banks
Major: Mechanical Engineering

The knowledge of glenohumeral joint contact force is crucial for reverse total shoulder arthroplasty (RTSA) surgery. It affects the stability of humerus during motions and the complication rate after the RTSA surgery. An instrumented implant was developed to measure three components of joint contact forces by four strain gauges. The accuracy of the instrumented implant is decided by the structure and the calibration method. Aims of this study were to develop a simple but accurate calibration method, to find a mathematical method for calculating forces from strain measurements, and to validate the intraoperative contact forces measurement was in a reliable range. Simple but accurate calibration method can be achieved by applying forces on 12 different poses of the calibration jig, which provided 12 sets of three linearly independent combinations of force components. The matrix method was used for force calculation from strain measurements, and most of the average measuring errors can be possibly kept below 6% of the calibration range. The instrumented implants were used in 3 patients in RTSA surgery, and strain data was measured during four passive motions. Joint reaction forces exhibited characteristic patterns that were consistent between three patients, and remained below 300 N for every passive motion. Highest joint

reaction force was found in 277 N during flexion. These first shown intraoperative measurements of glenohumeral joint contact forces are continuing with a goal of 20 total patients.

CHAPTER 1
INTRODUCTION

Reverse Total Shoulder Arthroplasty

In 2004, the U.S. Food and Drug Administration (FDA) released the reverse total shoulder arthroplasty (RTSA) to be used in specific clinical situations. The RTSA is a non-anatomic shoulder replacement, designed to provide a fixed fulcrum allowing the deltoid to elevate the arm. Recently, RTSAs are being increasingly recommended for patients who need a revision after previous surgery, or who suffer from massive rotator cuff tears (Figure 1-1-A,B) [1,2,3,4].

While the early outcomes of RTSA surgery are promising for improvements in range of motion and pain relief, the complication rate of RTSA is still high [5]. A significant early complication of RTSA is dislocation, occurring in up to 7.5% [6] of patients undergoing RTSA. It can occur due to multiple factors including scapula notching, neurological injury, periprosthetic fracture, baseplate failure, and acromion fracture [7]. Adequate tension of the deltoid is critical to prevent fractures and insure prosthesis stability. If the deltoid is insufficiently tensioned, it can lead to prosthesis dislocation (Figure 1-2); if the deltoid is over tensioned, it can result in an acromial fracture or neurovascular injury [8,9,10].

Soft-tissue Tension Measurement

Currently, there exists no scientific data regarding the optimal tension or “the tightness” that surgeons should follow when placing the RTSA prostheses. By using a sensor-instrumented femoral head, Tanino et al. [11] have recently obtained the intraoperative soft-tissue tension of the hip. The researchers were able to intraoperatively quantify soft-tissue tension and direction around the hip joint during

passive flexion and extension. The research team noted that intraoperative force direction changed significantly through the measured range of motion. Bergmann et al. have measured the glenohumeral joint contact forces of a patient 7 months after total shoulder arthroplasty by a telemetric instrumented implant [12], but no equivalent recordings have been performed for RTSA implants where the joint reaction forces are very likely different. A key goal of this research is to provide intraoperative joint-reaction force measurements in shoulders during RTSA surgery.

Various implants for measuring joint load and soft-tissue tension have been reported [13,14,15]. For multi-component force sensors, intraoperative measurements of each component of force are calculated from strain gauge signals using a calibration matrix method [16]. The calibration matrix method allows accurate force components to be determined from sensors with non-precisely positioned strain gauges, and was originally developed for three force components sensors [17,18].

There are two goals of this study: the first is to obtain objective data on the soft-tissue tension of shoulder joint during RTSA by using a custom designed instrumented implant; the second is to validate the calibration matrix method for computing joint-reaction forces from strain gauge readings.

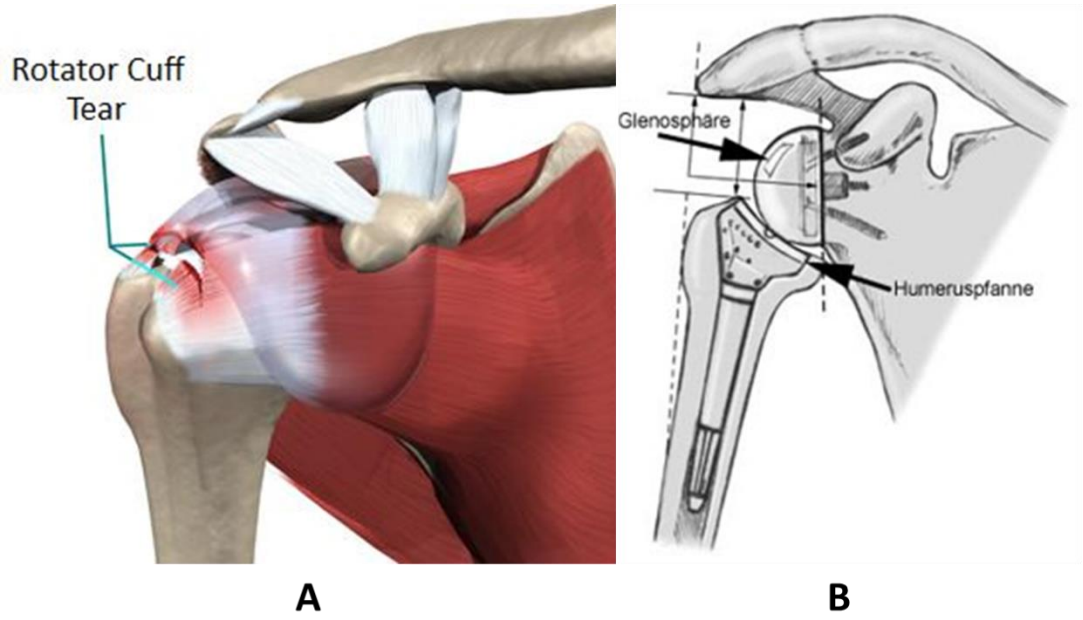

Figure 1-1. Rotator Cuff Tears and Reverse Total Shoulder Arthroplasty. A) Rotator Cuff Tears (Source: www.Healingartsce.com), B) Reverse Total Shoulder Arthroplasty (Source: www.Schulter.de/Endoprothetik)

Figure 1-2. Shoulder Joint Dislocation after RTSA surgery. (Source: Emilie Cheung, "Complication in Reverse Total Shoulder Arthroplasty", AAOS, 2011)

CHAPTER 2
MATERIALS AND METHODS

Instrumented Implant

There are several requirements for force instrumented implants [19]:

- The force-sensing implant should be designed according to the size of the standard RTSA prosthesis.
- The sensor must be compatible with the standard RTSA prostheses, should not affect their function, and its use should not significantly change the surgical procedure.
- The force-sensing implant must be sterilized before intraoperative use, and must not expose the patient to materials or interfaces that are not biocompatible.
- All three components of the shoulder joint reaction force should be measured with good accuracy.
- Strain gauges must be placed in an area of the implant where the entire joint load is transferred.

A custom designed instrumented implant was designed to fulfill these requirements (Figure 2-1-A,B). The implant was fabricated from 304 stainless steel and outfitted with four strain gauges (120 ohm uni-axial foil gauge, QFLG-2-11-1LJB, Tokyo Sokki Kenkyujo Co.,Ltd., Japan). The sensor was designed to fit within the modular glenosphere of a commercially available and FDA approved RTSA system (Equinoxe® Reverse Total Shoulder, Exactech Inc., Gainesville, FL). The four strain gauges are aligned with the implant post and glued in place (Figure 2-1-C). The strain gages are self-temperature compensated for 304 stainless steel over the temperature range including 20°C (room temperature) to 37°C (body temperature). Data acquisition was performed using USB-based data acquiisiotn hardware (NI-9219 DAQ, National Instruments, Austin, TX) and LabVIEW software (National Instruments). Calculation of the force components was performed with customized software.

Calibration

To achieve measurements with good accuracy, the setup of the calibration should be similar to the in-vivo situation. Therefore, the force-sensing implant is fixed on a custom jig, and a trial glenosphere is threaded on the stem of the implant. A polyethylene liner is arranged between load cell and the glenosphere (Figure 2-2-A), and calibration is performed by applying three linearly independent combinations of force components (Figure 2-2-A,B). A total of twelve different loading conditions are used for calibration (Figure 2-2-C). Forces F are applied at the same point, but the loading orientation is changed by manipulating the calibration jig. For example, when force applied at $elevation\ angle\ (\theta) = 30°$ and $rotation\ angle\ (\emptyset) = 60°$, the force vector is $F = [F_x = Fsin30°cos60°, F_y = Fsin30°sin60°, F_z = Fcos30°]$. The applied calibration forces were 10N, 20N, 40N, 70N, 100N, 200N, and 400N, in accordance with ASTM E4-08.

The relation between the applied forces and the signals from the four strain gauges can be written:

$$\begin{bmatrix} F_{x-applied} \\ F_{y-applied} \\ F_{z-applied} \end{bmatrix} = \begin{bmatrix} B_{11} & \cdots & B_{1n} \\ \vdots & \ddots & \vdots \\ B_{31} & \cdots & B_{3n} \end{bmatrix} \begin{bmatrix} S_{1-calibration} \\ S_{2-calibration} \\ S_{3-calibration} \\ S_{4-calibration} \end{bmatrix} \quad (1)$$

Where matrix B is the calibration matrix, which can be calculated as the pseudoinverse:

$$B = F_{applied} \times [{S_{calibration}}^T \left(S_{calibration} {S_{calibration}}^T\right)^{-1}] \quad (2)$$

To calculate Eq (2), four groups of different loading conditions are used for the calculation of the calibrationmatrix (Table 2-1). All of the constants in these calibration matrices are shown in Appendix B.

Table 2-1. The different angle-position combinations for the B matrix calculations

Group	Differ angle-position combinations	Number of angle positions
The 30°'s B Matrix	Ø=30°, -150°, -30°, 150°	4
The 45°'s B Matrix	Ø=45°, -135°, -45°, 135°	4
The 60°'s B Matrix	Ø=60°, -120°, -60°, 120°	4
The All12's B Matrix	Ø=30°, -150°, -30°, 150°, 45°, -135°, -45°, 135°, 60°, -120°, -60°, 120°	12

Calibration accuracy is quantified in terms of average relative errors, or residuals, of the load components i from all calibration measurements n:

$$e_{i-ave-cali.} = 100\% \times \sum \left| \frac{F_{i-calculated} - F_{i-applied}}{F_{i-max}} \right| / n \qquad (3)$$

where $F_{i-applied}$ is the known applied force component (i.e. $F_x = Fsin\theta°cos\emptyset°, F_y = Fsin\theta°sin\emptyset°, and\ F_z = Fcos\theta°$, when F=10N, 20N, 40N, 70N, 100N, 200N, and 400N), $F_{i-calculated}$ is the calculated force component:

$$\begin{bmatrix} F_{x-calculated} \\ F_{y-calculated} \\ F_{z-calculated} \end{bmatrix} = \begin{bmatrix} B_{11} & \cdots & B_{14} \\ \vdots & \ddots & \vdots \\ B_{31} & \cdots & B_{34} \end{bmatrix} \times \begin{bmatrix} S_{1-calibration} \\ S_{2-calibration} \\ S_{3-calibration} \\ S_{4-calibration} \end{bmatrix} \qquad (4)$$

and F_{i-max} is the calibration range of component i. Bergmann et al. [16] classified instrumented implants with a maximum error below 2% as "very accurate," below 4% as "accurate," below 10% as "inaccurate," and above 10% as "very inaccurate."

Intraoperative Measurements

The instrumented implants were used in 3 patients (p#11, p#12, and p#13) during RTSA surgery, and were removed immediately after the intraoperative measurements. Four passive motions – external rotation, flexion, scaption, and abduction – were tested while recording the strain measurements. Additional patient

studies are continuing with a goal of 20 total patients with intraoperative measurement of shoulder joint reaction forces.

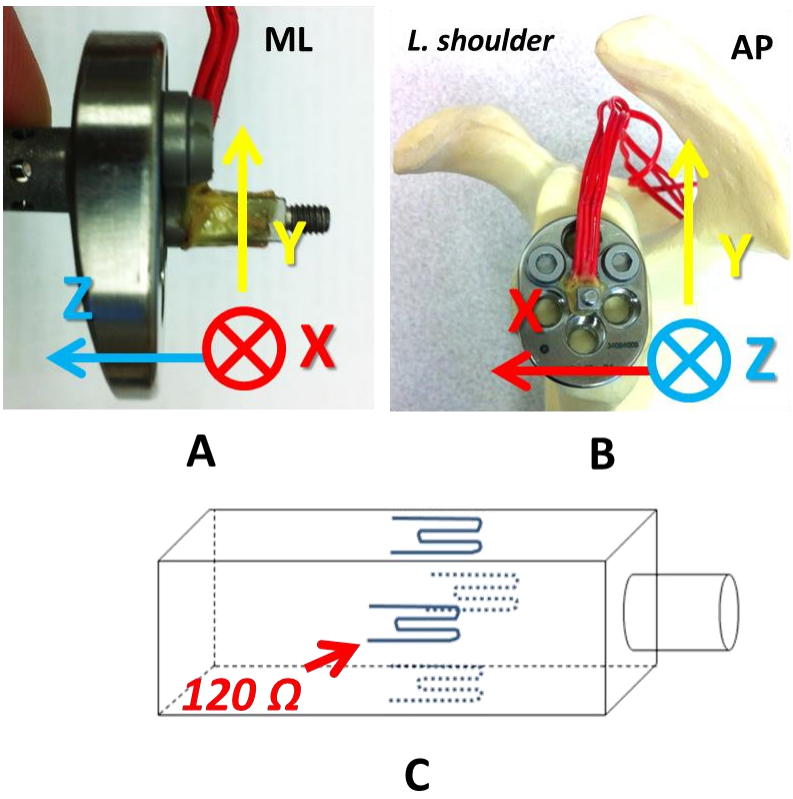

Figure 2-1. The Custom Designed Instrumented Implant. A) The medial-lateral view of the implant. B) The anterior-posterior view of the implant. C) The four strain gauges are aligned with the implant post and glued in place.

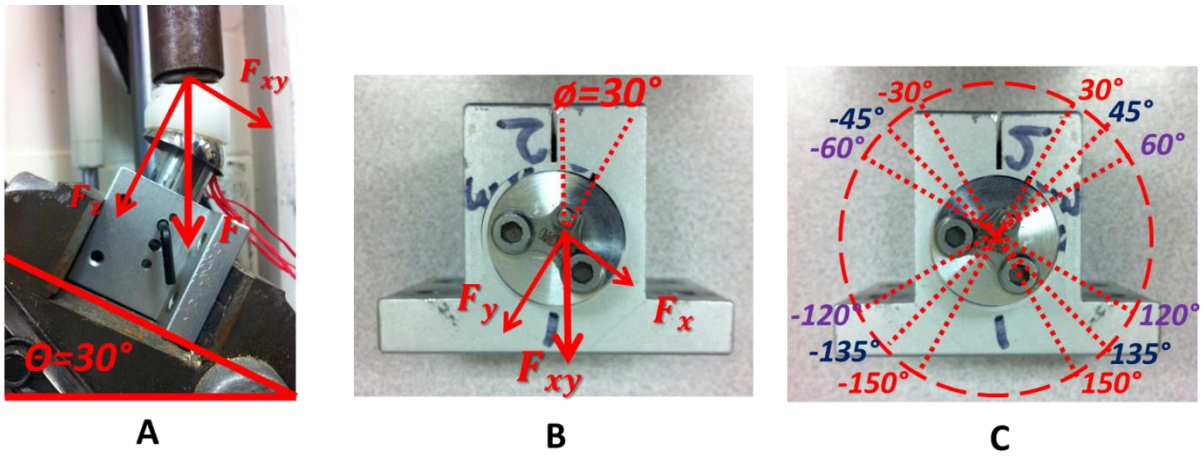

Figure 2-2. The Calibration Jig; A) is rotated 30 degrees about X-axis, B) is rotated 30 degrees about Z-axis, C) can be used for 12 different loading conditions.

CHAPTER 3
CALIBRATION RESULTS

Linearity of the Strain Measurement

The force-strain response was linear for most stain gauges and for most sensor orientations (Figure 3-1, Tables 3-1, 3-2, 3-3, Appendix A). However, each sensor exhibited instances of individual gauges at specific orientations where the force-strain response was nonlinear (Figures 3-2, 3-3, 3-4).

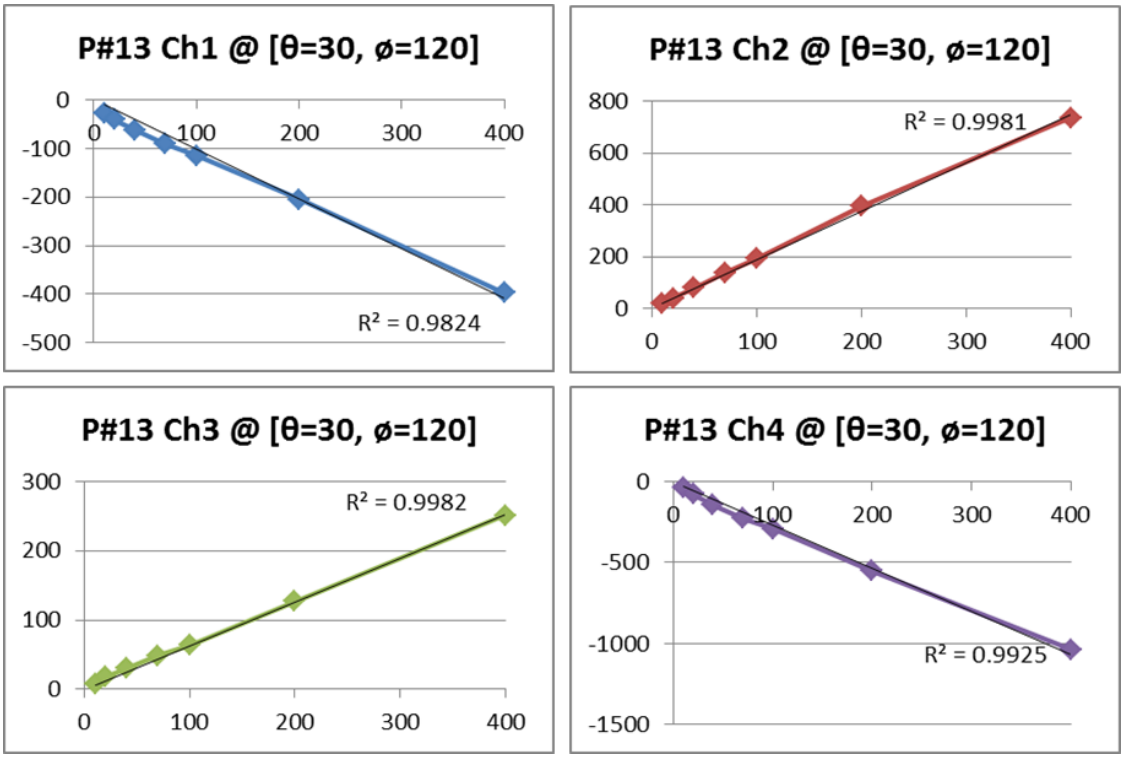

Figure 3-1. Linear strain measurement during calibration (X-axis: Applied force (N); Y-Axis: Strain (με))

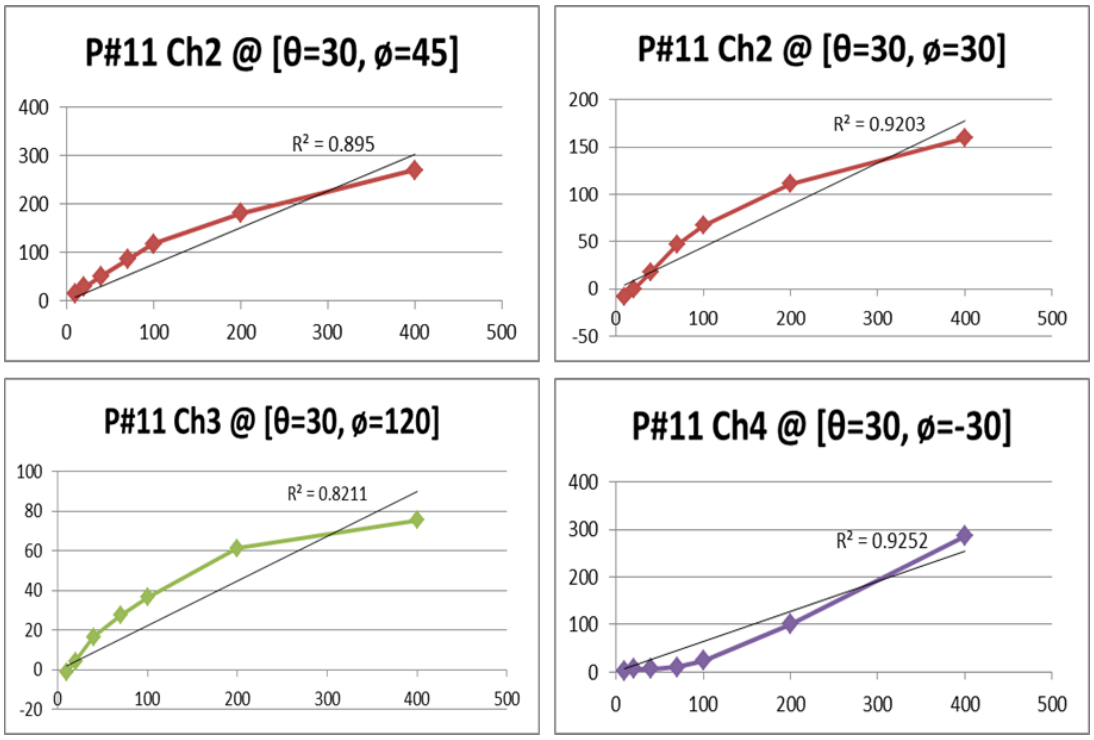

Figure 3-2. Strain measurement during calibration showed nonlinearity in some sensors in patient #11 (X-axis: Applied force (N); Y-Axis: Strain (με))

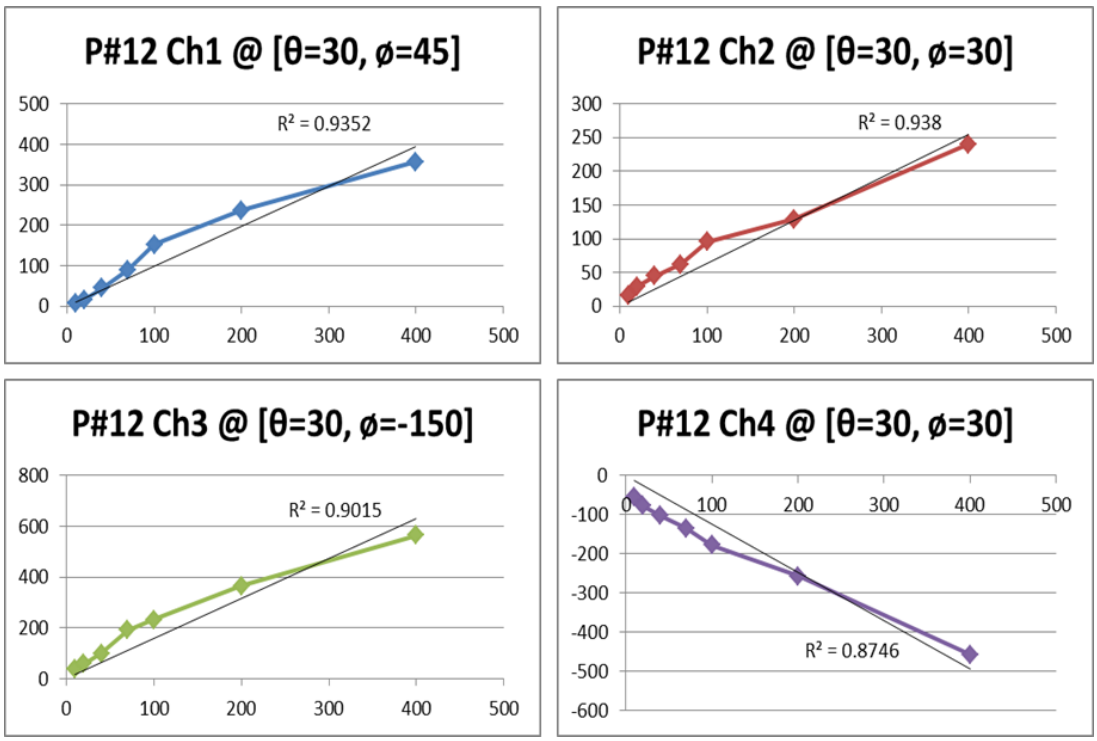

Figure 3-3. Strain measurement during calibration showed nonlinearity in some sensors in patient #12 (X-axis: Applied force (N); Y-Axis: Strain (με))

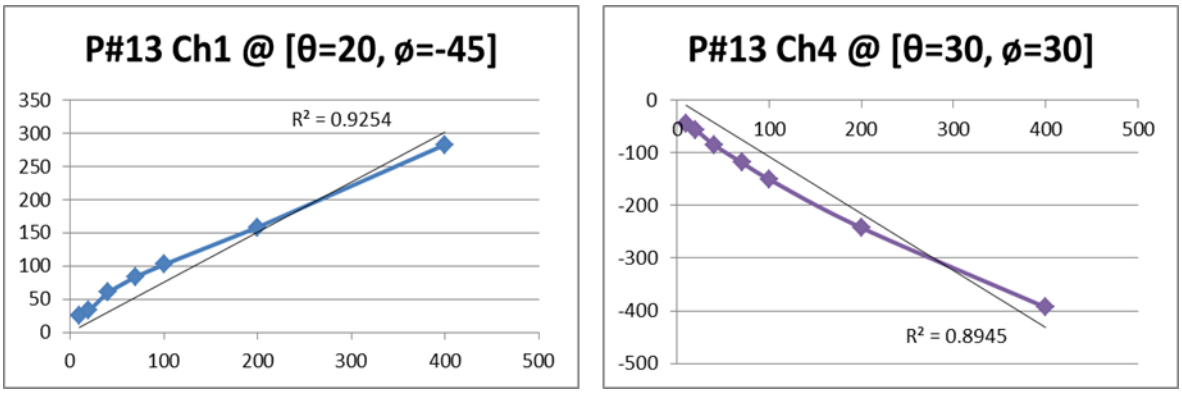

Figure 3-4. Strain measurement during calibration showed nonlinearity in some sensors in patient #13 (X-axis: Applied force (N); Y-Axis: Strain (με))

Linear Calibration

A highly linear response for F_x and F_y (R^2>0.99) was noted between calculated and applied forces (Figure 3-5, 3-6, 3-7). However, a high coefficient of determination (R^2) does not necessarily indicate good measurement accuracy [12], because occasional high errors will only decrease R^2 slightly. The relative errors of load components i from each calibration measurement:

$$e_{i-cali.} = 100\% \times \left| \frac{F_{i-calculated} - F_{i-applied}}{F_{i-max}} \right| \qquad (5)$$

where the definition of $F_{i-calculated}$, $F_{i-applied}$, and F_{i-max} is the same as in Eq. (3); $F_{i-calculated}$ were computed by the All12's B Matrix (Table 2-1)

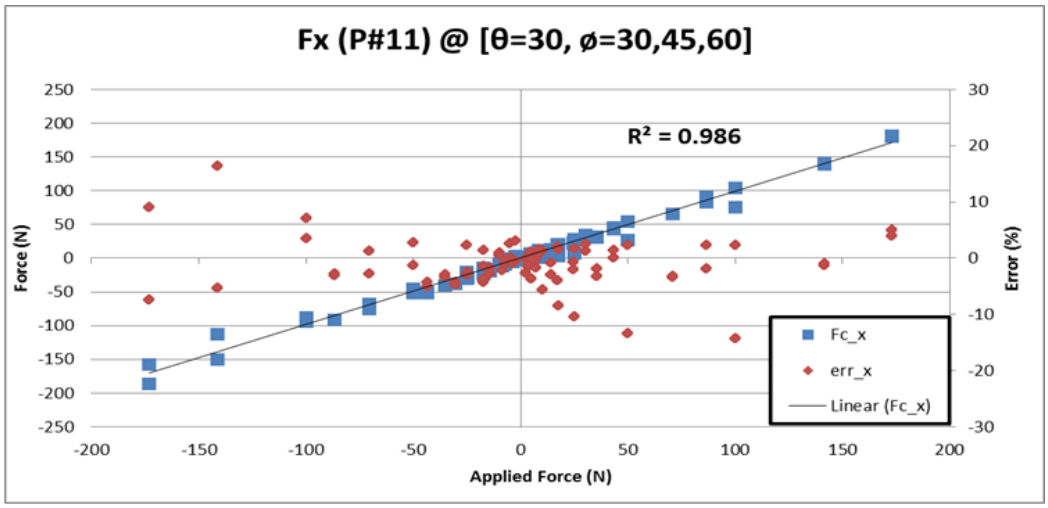

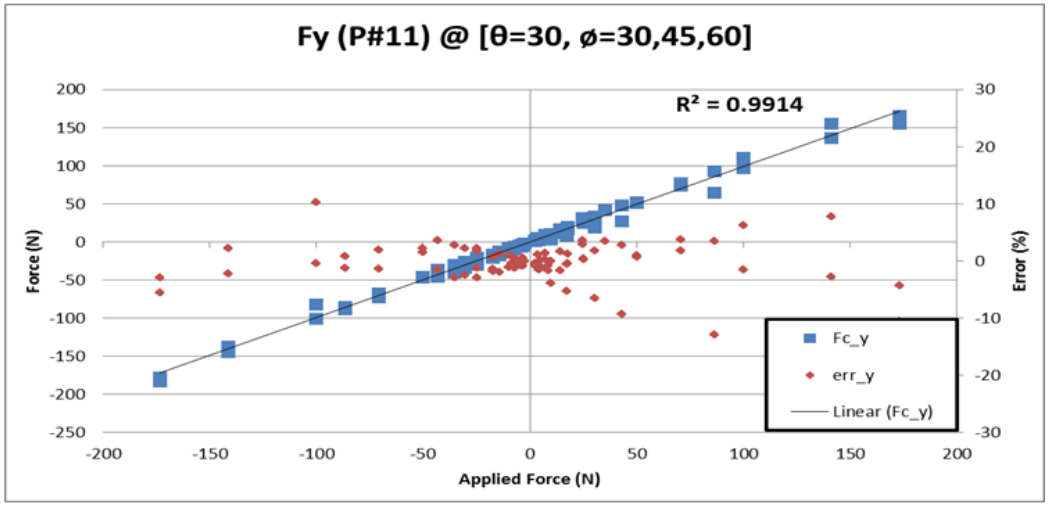

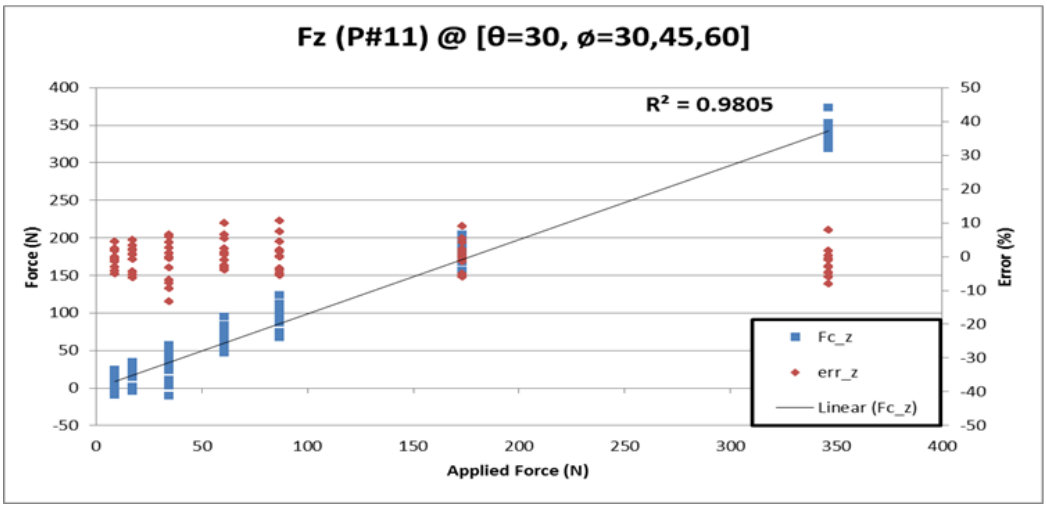

Figure 3-5. Linear response of the strain measurement according to corresponding applied forces during calibration in patient #11 (X-axis: Applied force (N); Left vertical axis: Calculated force (N); Right vertical axis: the relative errors (%))

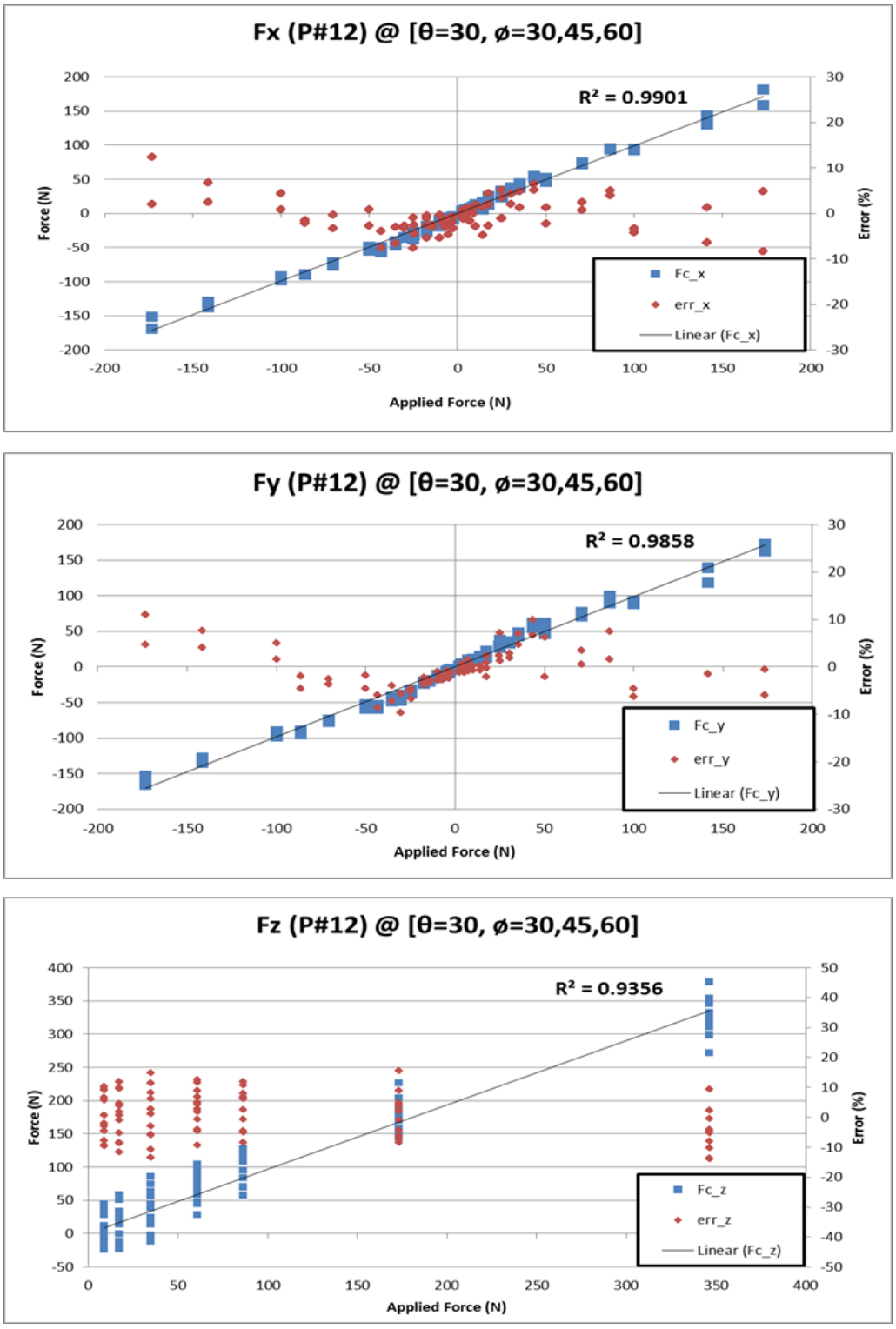

Figure 3-6. Linear response of the strain measurement according to corresponding applied forces during calibration in patient #12 (X-axis: Applied force (N); Left vertical axis: Calculated force (N); Right vertical axis: the relative errors (%))

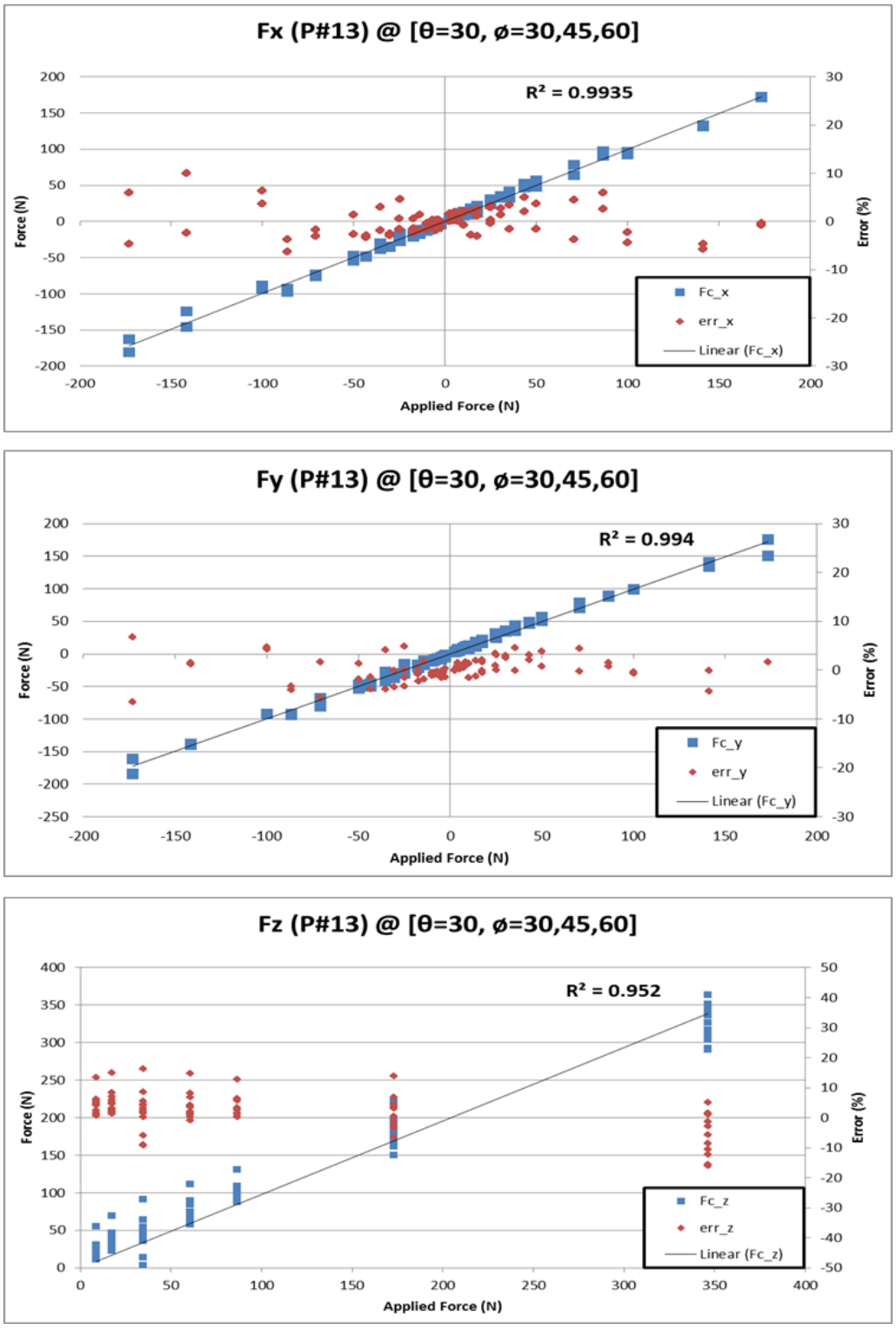

Figure 3-7. Linear response of the strain measurement according to corresponding applied forces during calibration in patient #13 (X-axis: Applied force (N); Left vertical axis: Calculated force (N); Right vertical axis: the relative errors (%))

Calibration and Measuring Error

Using different combinations of applied force (Table 2-1) affected the calibration residual errors (Tables 3-1). In general, calibration performed with a total of four different loading orientations resulted in smaller average residual errors than calibrations using the entire set of twelve loading orientations.

Table 3-1. The calibration errors of each calibration matrix

Patient number	Calibration matrix	$e_{x,ave}$	$e_{y,ave}$	$e_{z,ave}$
Patient #11	The 30°'s B Matrix	5.228	2.537	4.000
	The 45°'s B Matrix	2.975	1.904	2.743
	The 60°'s B Matrix	2.309	2.478	2.403
	The All12's B Matrix	3.933	2.717	3.393
Patient #12	The 30°'s B Matrix	3.694	3.759	6.032
	The 45°'s B Matrix	2.439	4.314	3.420
	The 60°'s B Matrix	2.335	4.323	4.981
	The All12's B Matrix	3.497	4.161	6.625
Patient #13	The 30°'s B Matrix	2.585	2.179	6.602
	The 45°'s B Matrix	2.916	2.283	3.957
	The 60°'s B Matrix	2.197	1.902	3.361
	The All12's B Matrix	2.751	2.320	4.663

CHAPTER 4
IN-VIVO MEASUREMENT OF SHOULDER JOINT CONTACT FORCES

Intraoperative joint reaction forces were calculated from the intraoperative strain measurements and the sensor calibration matrix as described previously in Eq (4):

$$\begin{bmatrix} F_{x-react} \\ F_{y-react} \\ F_{z-react} \end{bmatrix} = \begin{bmatrix} B_{11} & \cdots & B_{14} \\ \vdots & \ddots & \vdots \\ B_{31} & \cdots & B_{34} \end{bmatrix} \times \begin{bmatrix} S_{1-intraoperative} \\ S_{2-intraoperative} \\ S_{3-intraoperative} \\ S_{4-intraoperative} \end{bmatrix} \quad (6)$$

where $S_{intraoperative}$ is the intraoperative measurement of strain, B is the linear sensor calibration matrix, and F_{react} is the computed joint reaction force vector.

Intraoperative joint reaction force components were computed using the All12's B matrix (Table 2-1). The maximum joint force components during passive arm motions are shown in Table 4-1 and 4-2.

Table 4-1. The highest forces during each passive motion for each patient (units in Newton)

	Patient #11				Patient #12				Patient #13			
	F_x	F_y	F_z	F_{res}	F_x	F_y	F_z	F_{res}	F_x	F_y	F_z	F_{res}
Starting position	100	70	125	175	-10	45	40	65	-10	70	25	75
External Rotation	154	70	170	223	-20	69	53	76	15	88	38	91
Flexion	195	90	228	277	-22	69	89	90	-52	90	70	122
Scaption	114	104	160	209	-18	63	60	86	10	94	55	97
Abduction	148	109	170	220	-30	56	57	77	89	89	90	130

Note: units in Newton (N)

Table 4-2. The highest forces during each passive motion in each patient (units in percentage of bodyweight)

	Patient #11				Patient #12				Patient #13			
	F_x	F_y	F_z	F_{res}	F_x	F_y	F_z	F_{res}	F_x	F_y	F_z	F_{res}
Starting position	13	9	16	22	-1	6	5	8	-1	9	3	9
External Rotation	19	9	21	28	-3	9	7	10	2	11	5	11
Flexion	24	11	29	35	-3	9	11	11	-7	11	9	15
Scaption	14	13	20	26	-2	8	8	11	1	12	7	12
Abduction	19	14	21	28	-4	7	7	10	11	11	11	16

Note: units in percentage of bodyweight (BW%)

External Rotation

During passive external/internal rotation, the surgeon moved the arms of the patients from 0° to 90° external rotation while supporting the arm against gravity. Maximum joint reaction forces were 223 N in patient #11 (Figure 4-1), 76 N in patient #12 (Figure 4-2), and 91 N in patient #13 (Figure 4-3). In patient #13 the z-component of force was transiently negative, indicating the joint was under tension. This is not physically possible, and must result from measurement noise or calibration errors. .

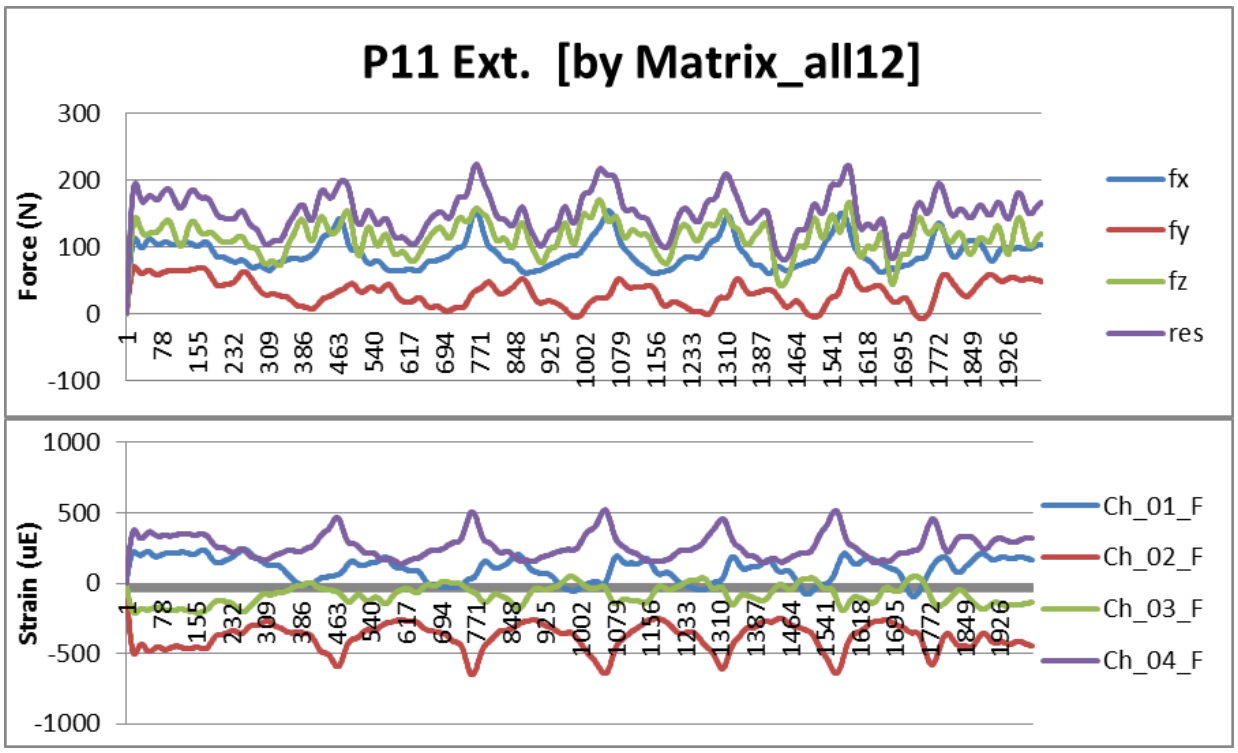

Figure 4-1. In-vivo measurement of external rotation for patient #11 (Upper: Calculated Intraoperative Joint Contact Forces; Lower: Strain measurement)

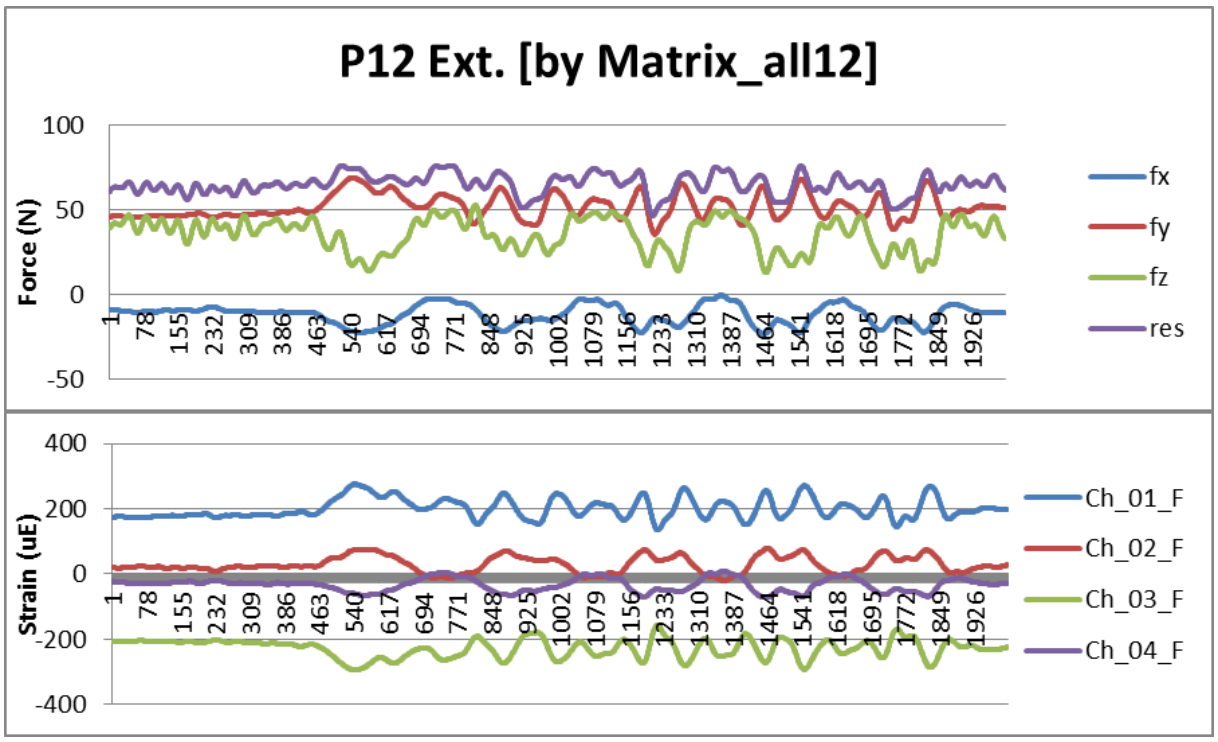

Figure 4-2. In-vivo measurement of external rotation for patient #12 (Upper: Calculated Intraoperative Joint Contact Forces; Lower: Strain measurement)

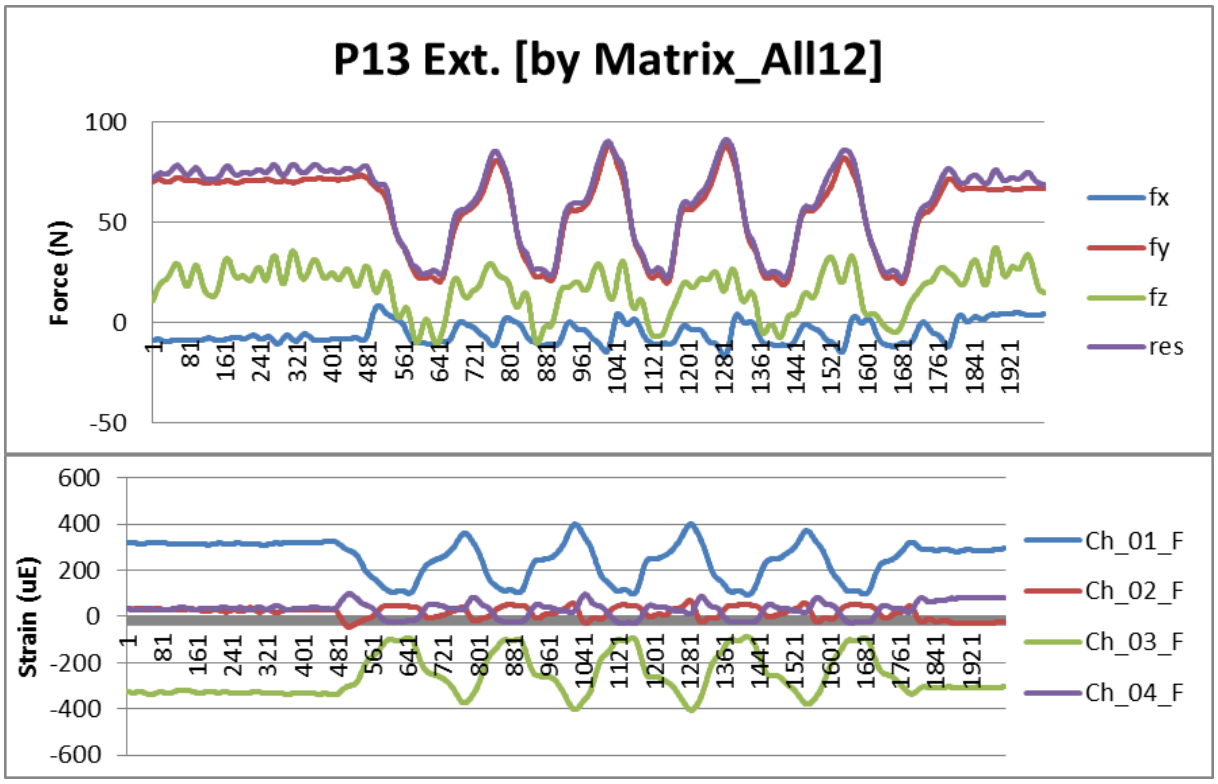

Figure 4-3. In-vivo measurement of external rotation for patient #13 (Upper: Calculated Intraoperative Joint Contact Forces; Lower: Strain measurement)

Flexion

During the passive flexion motion, the surgeon raised the patients' arms up to 90° while supporting them against gravity. The maximum calculated joint reaction forces were 277 N in patient #11 (Figure 4-4), 90 N in patient #12 (Figure 4-5), and 122 N in patient# 13 (Figure 4-6). These values are higher than for external rotation, indicating a larger component of arm weight acting at the joint.

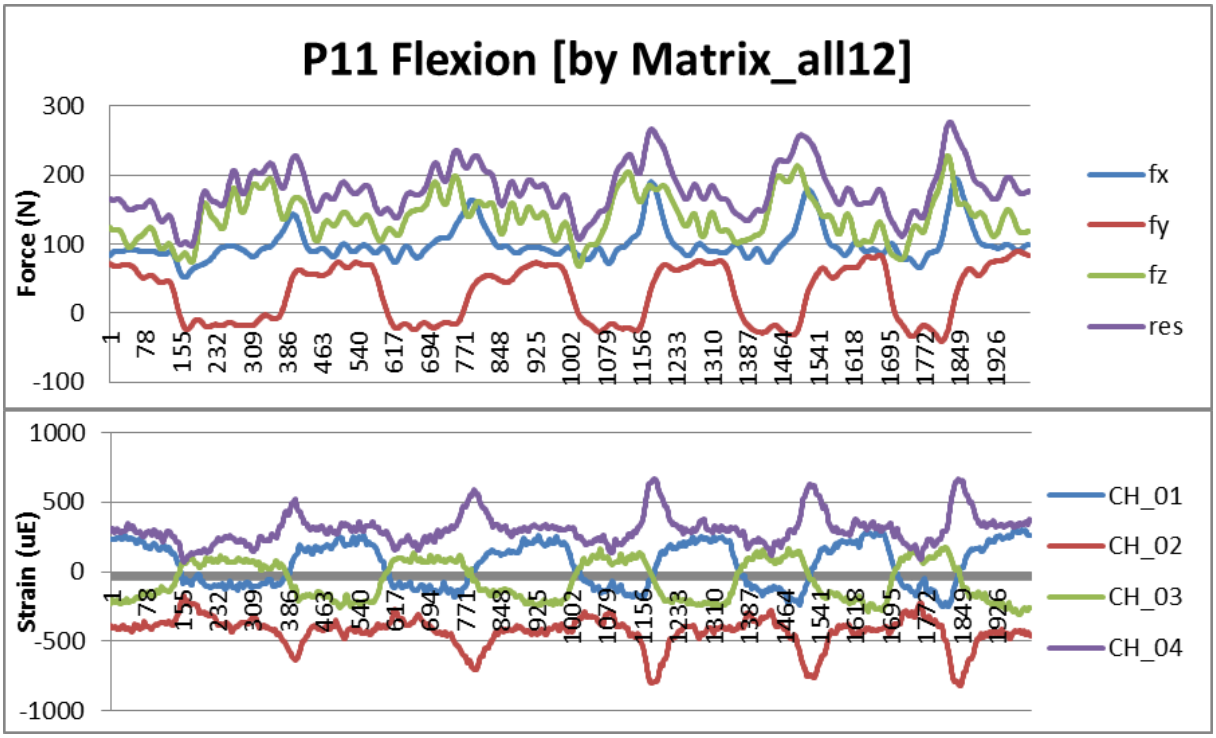

Figure 4-4. In-vivo measurement of flexion for patient #11 (Upper: Calculated Intraoperative Joint Contact Forces; Lower: Strain measurement)

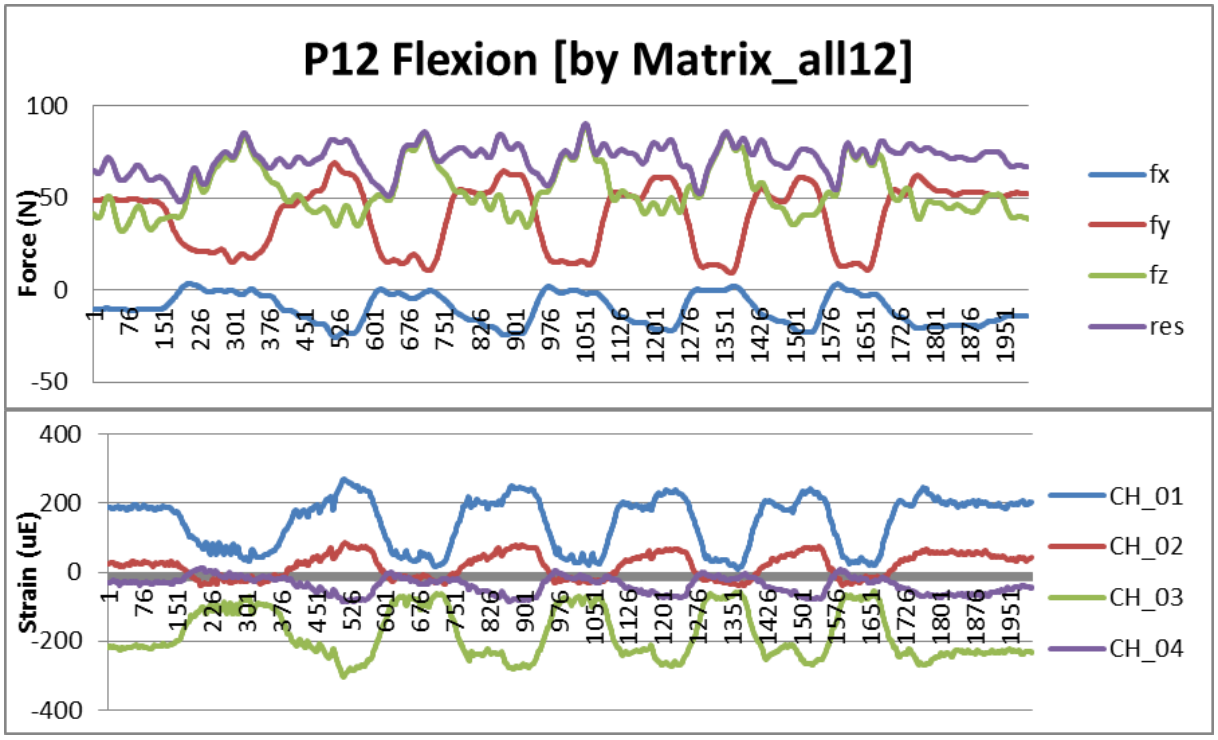

Figure 4-5. In-vivo measurement of flexion for patient #12 (Upper: Calculated Intraoperative Joint Contact Forces; Lower: Strain measurement)

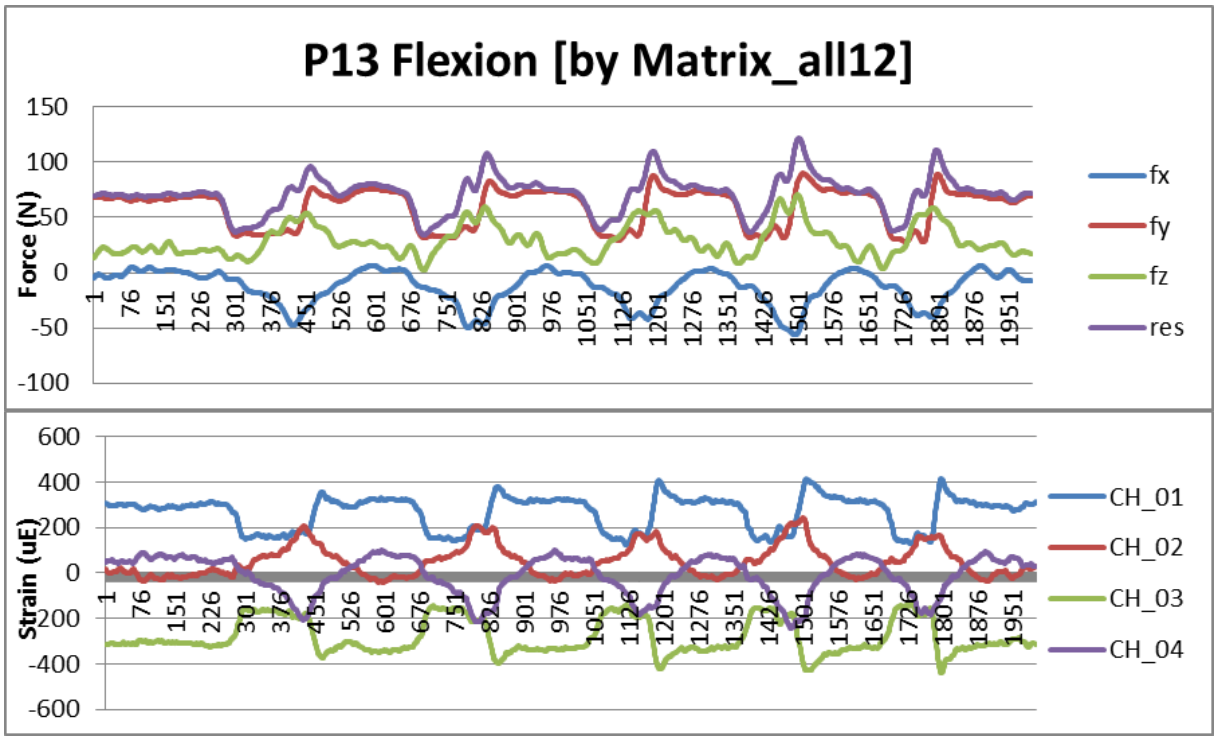

Figure 4-6. In-vivo measurement of flexion for patient #13 (Upper: Calculated Intraoperative Joint Contact Forces; Lower: Strain measurement)

Scaption

Passive scaption motion was performed from the arm at the side to 90°, and maximum joint reaction forces were 209 N in patient #11 (Figure 4-7), 86 N in patient #12 (Figure 4-8), and 97 N in patient# 13 (Figure 4-9).

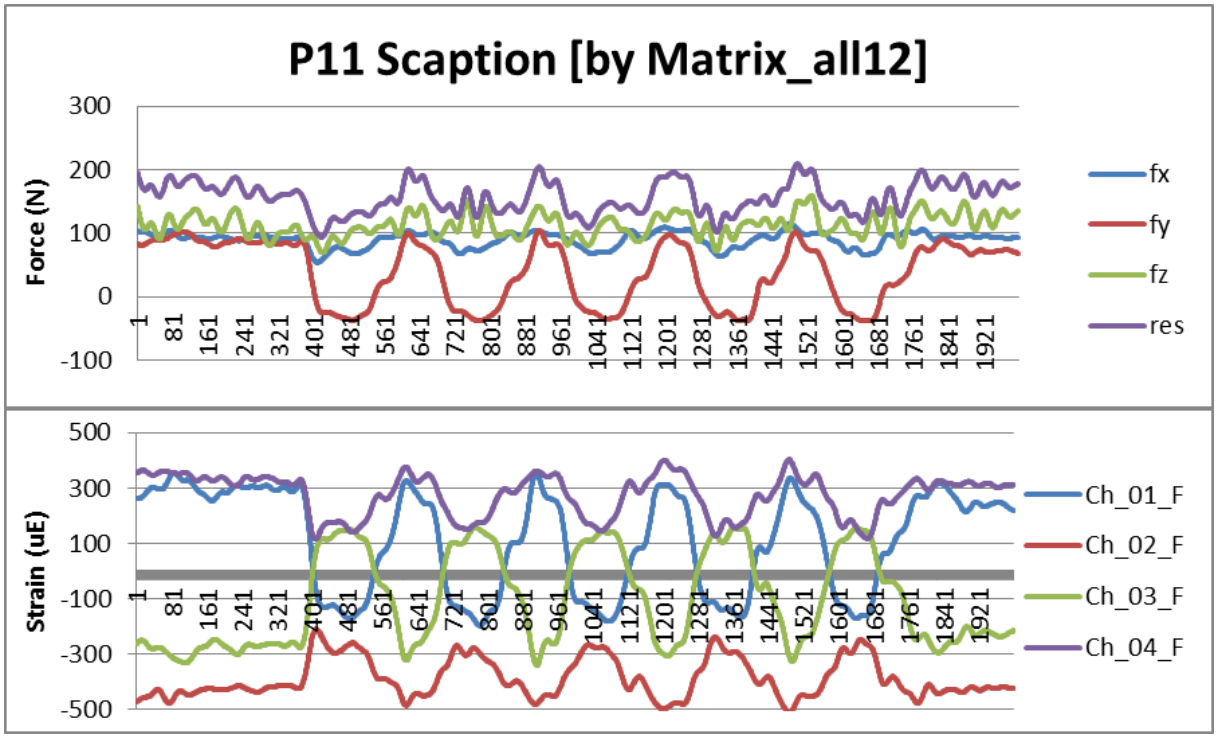

Figure 4-7. In-vivo measurement of scaption for patient #11 (Upper: Calculated Intraoperative Joint Contact Forces; Lower: Strain measurement)

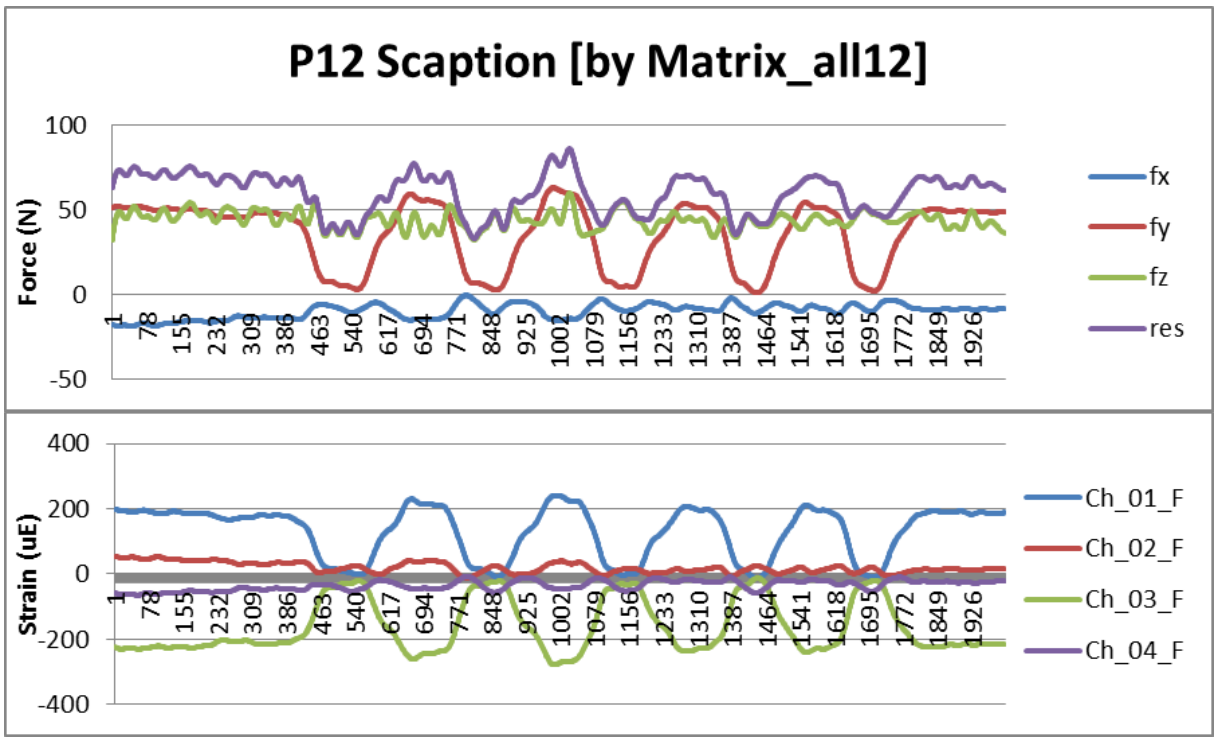

Figure 4-8. In-vivo measurement of scaption for patient #12 (Upper: Calculated Intraoperative Joint Contact Forces; Lower: Strain measurement)

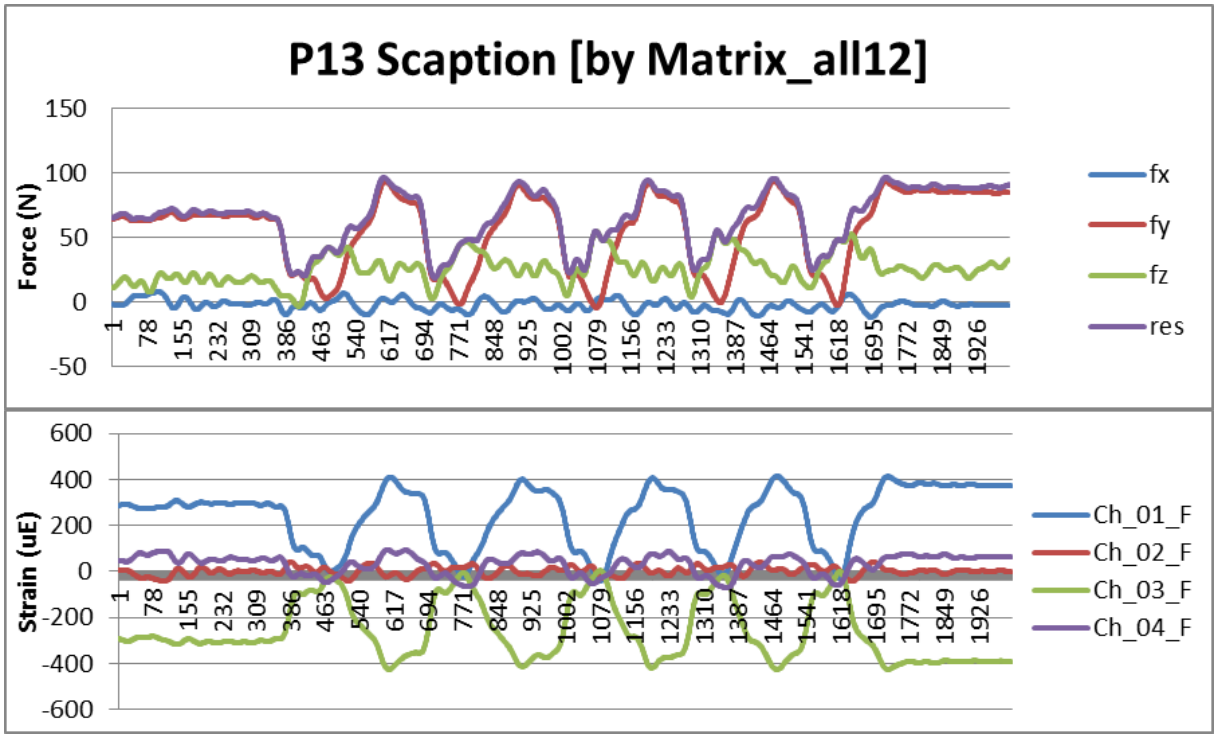

Figure 4-9. In-vivo measurement of scaption for patient #13 (Upper: Calculated Intraoperative Joint Contact Forces; Lower: Strain measurement)

Abduction

Passive abduction of the arm was performed from 0° to 90° with the arm in a plane parallel to the ground. Maximum joint reaction forces were 220 N in patient #11 (Figure 4-10), 77 N in patient #12 (Figure 4-11), and 130 N in patient# 13 (Figure 4-12).

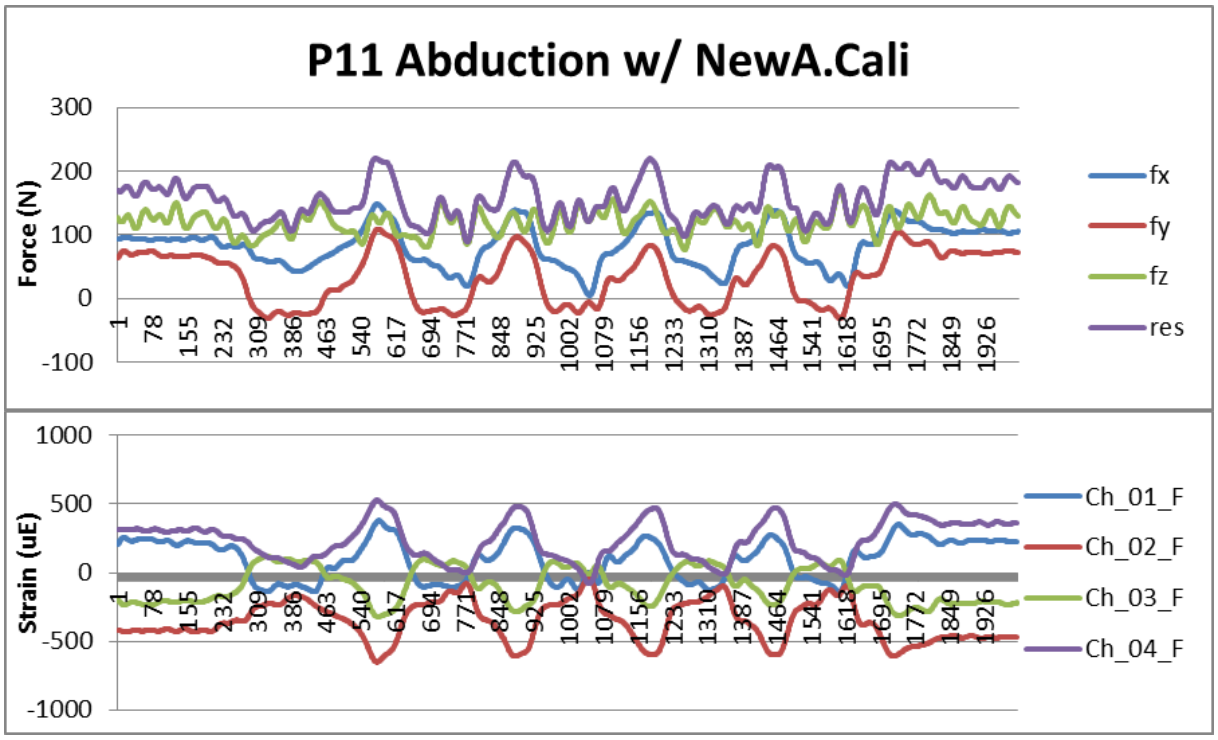

Figure 4-10. In-vivo measurement of abduction for patient #11 (Upper: Calculated Intraoperative Joint Contact Forces; Lower: Strain measurement)

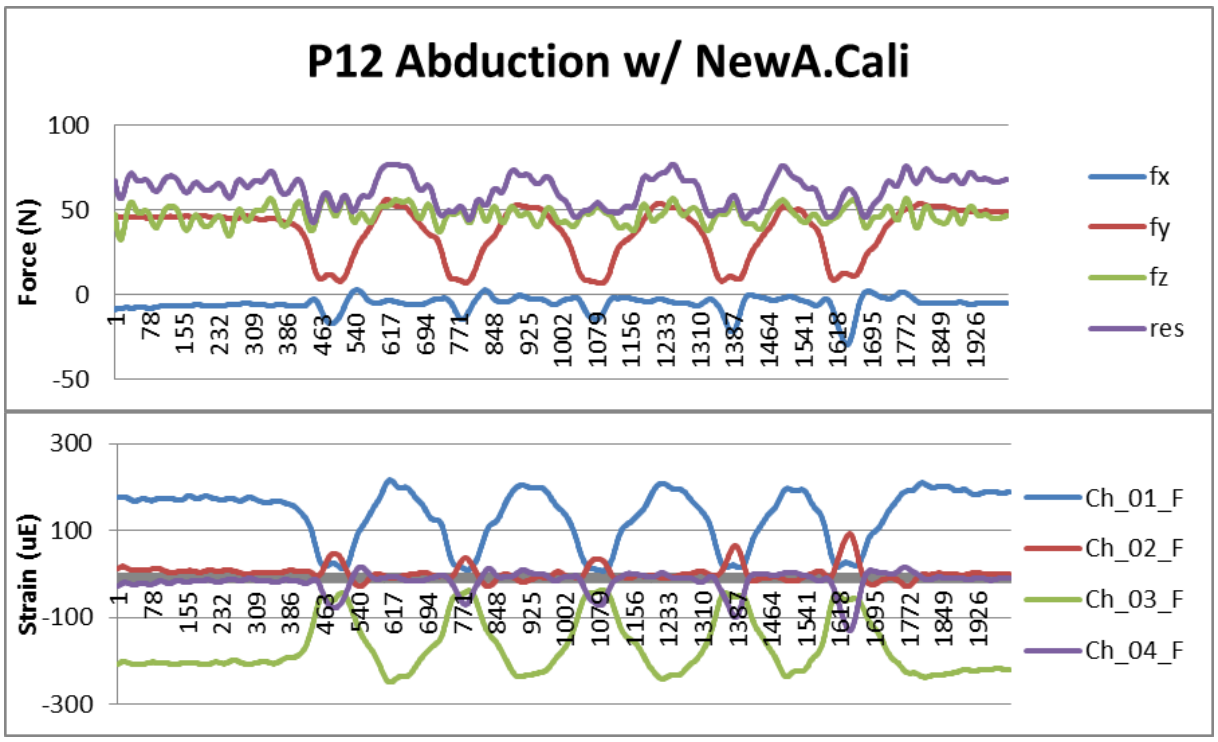

Figure 4-11. In-vivo measurement of abduction for patient #12 (Upper: Calculated Intraoperative Joint Contact Forces; Lower: Strain measurement)

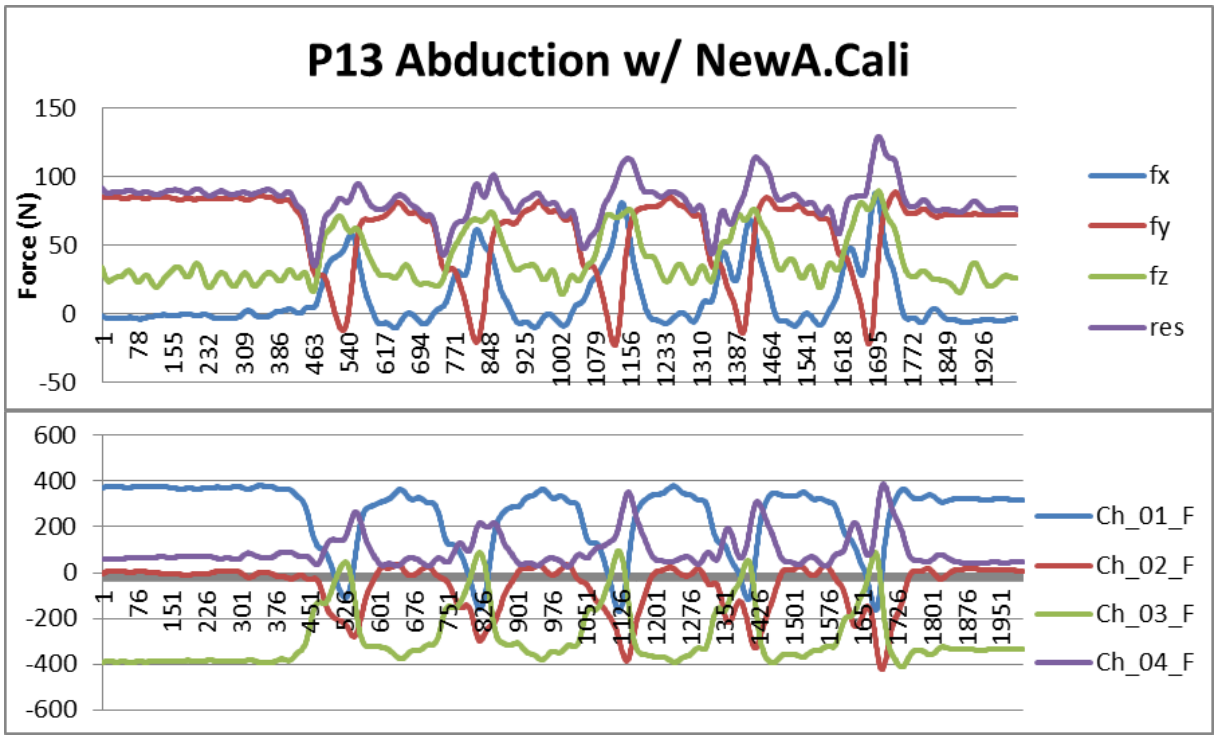

Figure 4-12. In-vivo measurement of abduction for patient #13 (Upper: Calculated Intraoperative Joint Contact Forces; Lower: Strain measurement)

CHAPTER 5
CONCLUSION

Understanding the soft-tissue tension during Reverse Total Shoulder Arthroplasty (RTSA) is critical to the success of the surgery. The studies discussed in Chapter 3 and Chapter 4 aimed to provide the intraoperative force measurement during passive motions. These results were validated by the calibration described in Chapter 3 which provides an accurate method to calculate the joint reaction force vector from the intraoperative strain measurements.

In Chapter 3, it was found that the strain measurement of each sensor of each implant is close to linear with respect to the applied forces. According to the linearity of the strain measurement, the calibration matrix-method is then applied to calculate the forces from strain measurements. The average relative errors between the applied forces and the forces recalculated using the calibration matrix are less than 6%. Different calibration errors were found by applying different sets of loading conditions and calculating the calibration matrix. This might because of experimental issues, including inaccurate machining of the custom calibration jig or slightly different load application conditions during calibration. Nevertheless, these results provide satisfactory demonstration of the calibration matrix method for calculating the intraoperative joint reaction forces from sensor strain measurements.

In Chapter 4, it was found that intraoperative joint reaction forces exhibited characteristic patterns that were consistent between three patients. However, the absolute level of force was quite different between the patients, indicating different levels of soft-tissue tension in each shoulder (or unaccounted differences in the sensors used).

In conclusion, a reliable calibration method has been developed for the intraoperative shoulder joint contact force measurement during RTSA. Further refinements in the calibration procedure, primarily more accurate fixturing, may result in more accurate calibration and joint force measurements.

APPENDIX A
LINEARITY OF THE STRAIN MEASUREMENT

Strain Measurements of calibration for each sensor from each implant:

Implant for Patient 11:

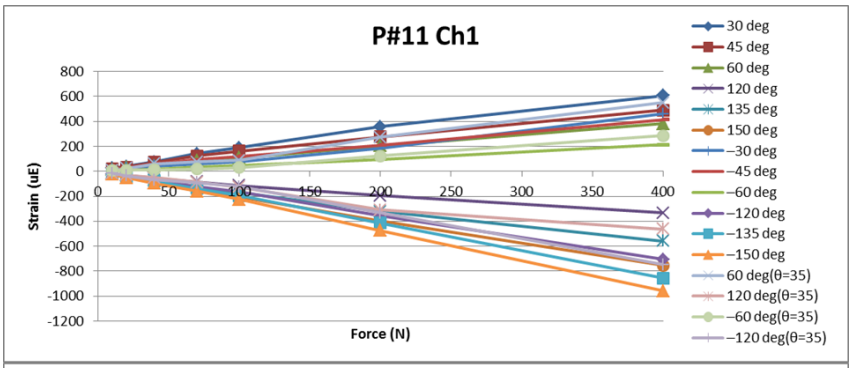

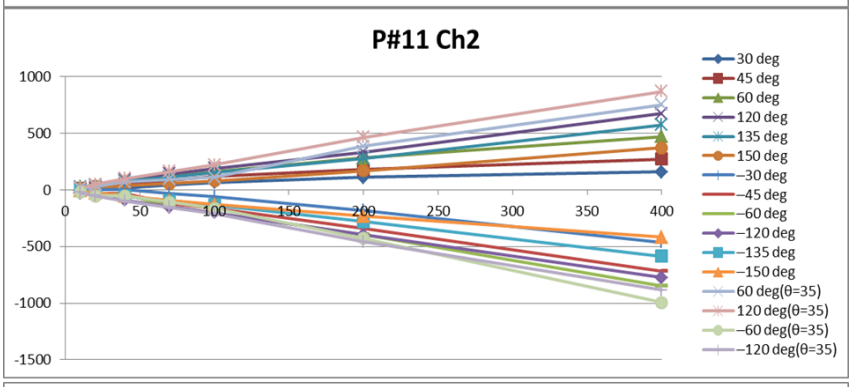

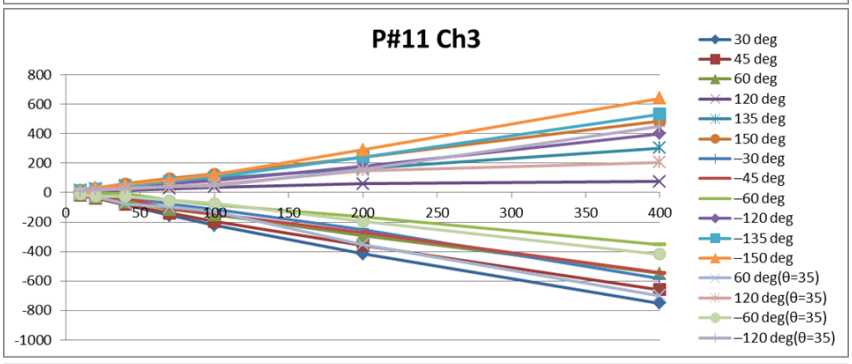

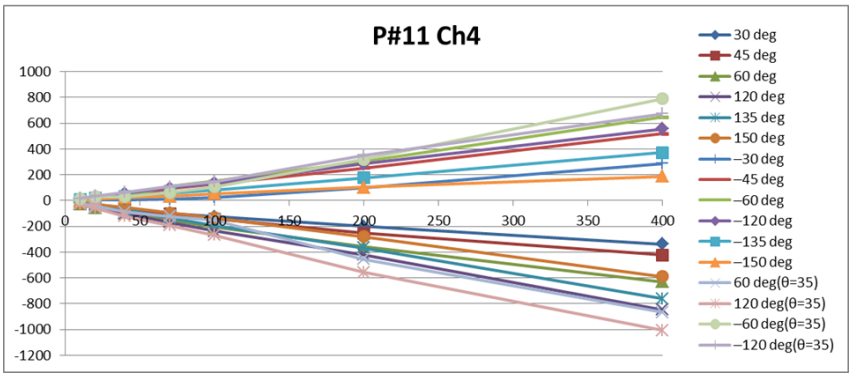

Implant for patient 12:

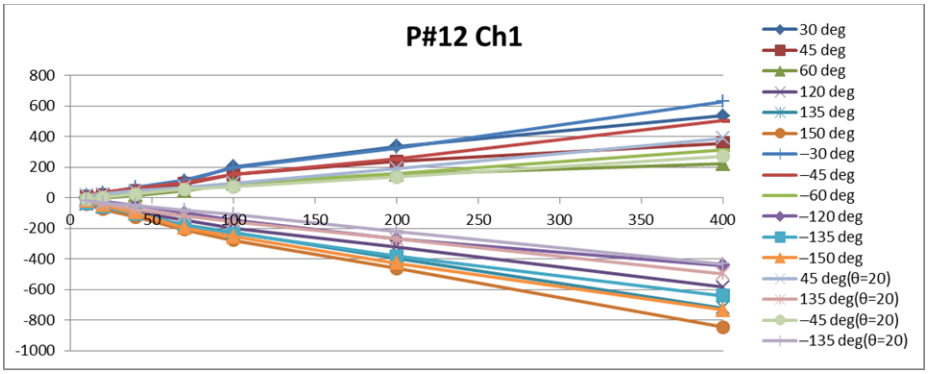

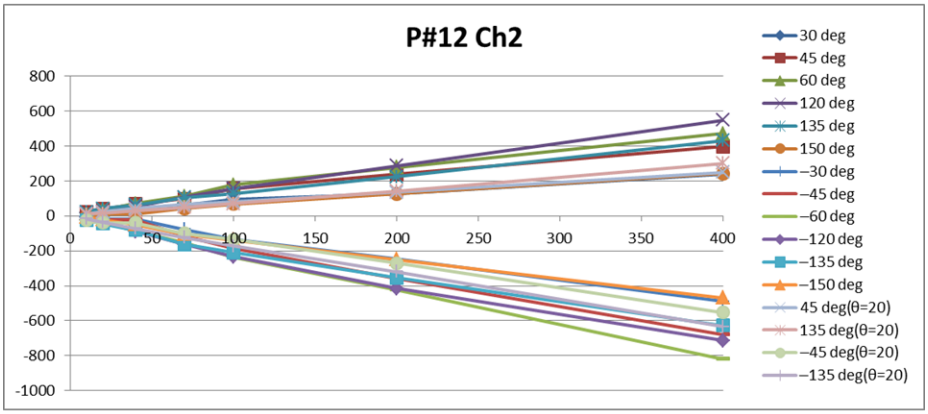

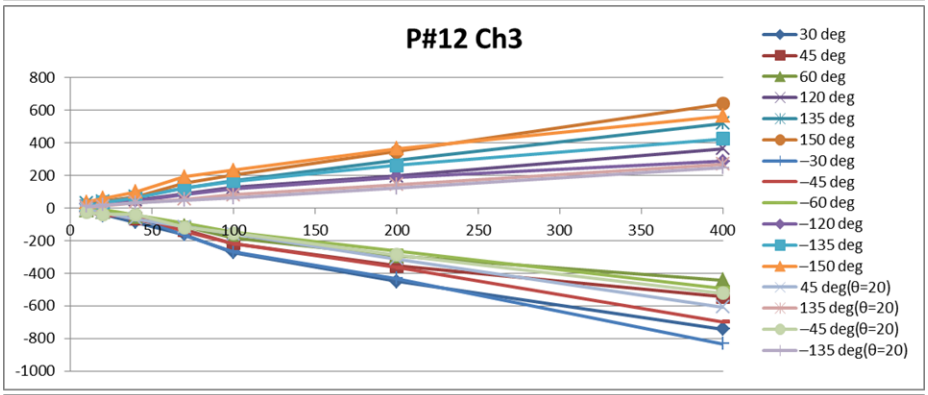

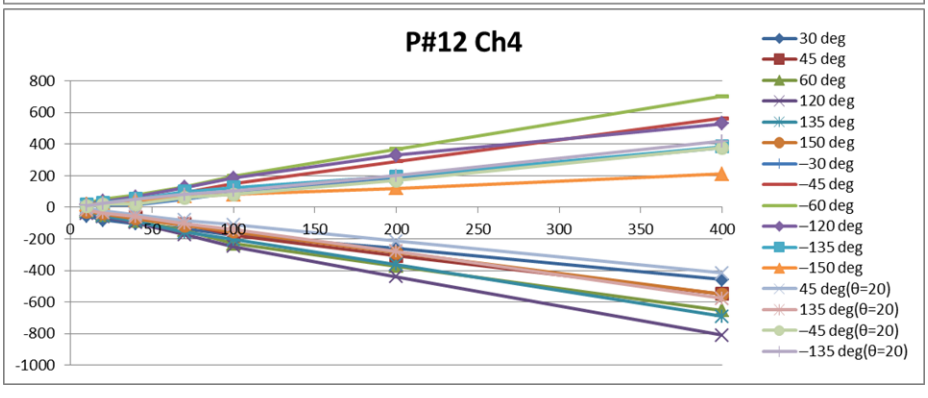

Implant for patient 13:

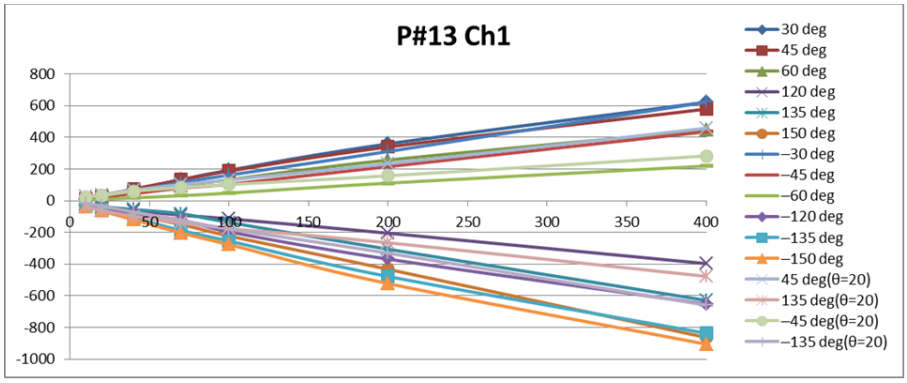

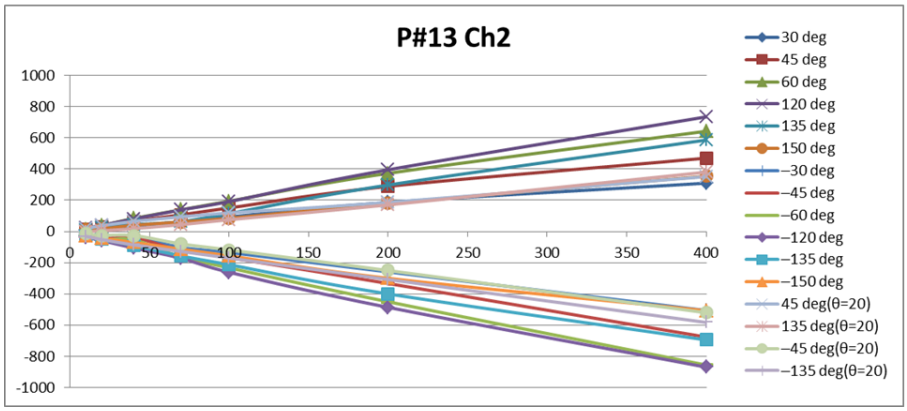

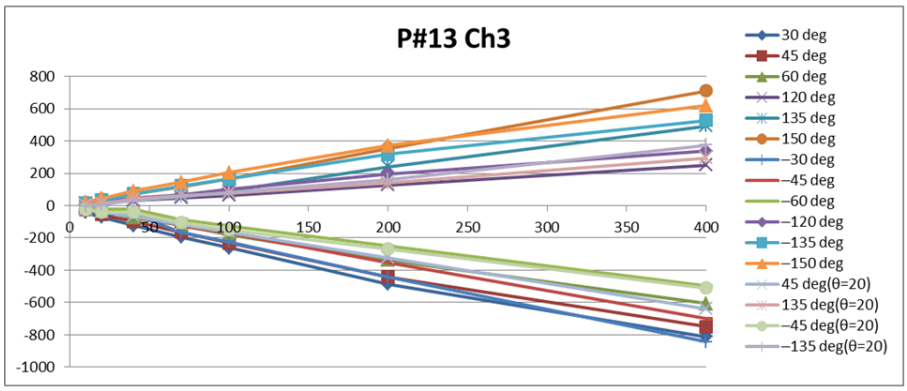

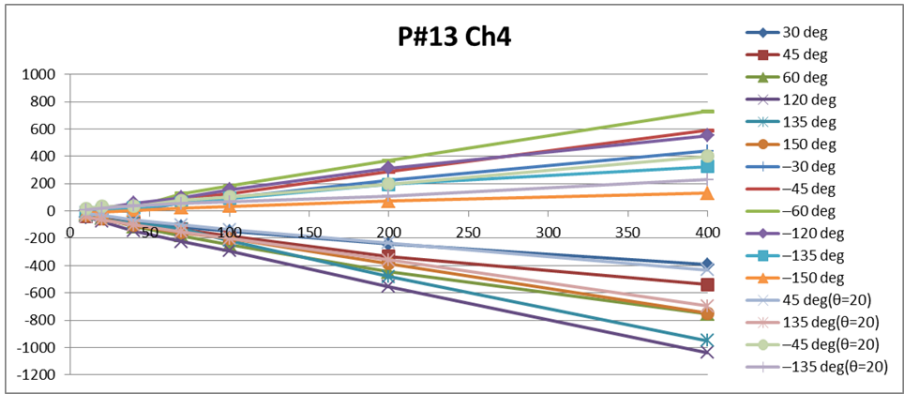

APPENDIX B
CONSTANTS IN CALIBRATION MATRICES

	Calibration Configurations	**Constants in Matrix B** (Calibration Matrix)			
Patient #11 (θ=30°)	**The 30°'s B Matrix**	0.109	-0.286	0.145	-0.014
		0.068	-0.031	-0.198	0.033
		-0.708	-0.867	-0.845	-0.876
	The 45°'s B Matrix	0.197	-0.385	0.270	-0.140
		-0.020	0.144	-0.284	0.192
		-0.453	-1.259	-0.562	-1.295
	The 60°'s B Matrix	0.204	-0.377	0.277	-0.148
		-0.016	0.148	-0.290	0.206
		-0.236	-1.474	-0.336	-1.509
	The All12's B Matrix	0.100	-0.274	0.147	-0.047
		0.221	-0.144	-0.009	-0.111
		-0.478	-1.168	-0.599	-1.201
Patient #12 (θ=30°)	**The 30°'s B Matrix**	0.127	-0.242	0.125	0.018
		0.103	0.013	-0.132	-0.004
		-0.460	-1.114	-0.519	-0.958
	The 45°'s B Matrix	-0.131	0.026	-0.097	0.279
		0.226	-0.136	-0.030	-0.155
		-0.474	-1.172	-0.619	-1.180
	The 60°'s B Matrix	-0.320	0.233	-0.247	0.482
		0.295	-0.213	0.031	-0.221
		0.007	-1.770	-0.147	-1.664
	The All12's B Matrix	0.055	-0.166	0.065	0.087
		0.108	-0.008	-0.130	-0.022
		-0.862	-0.778	-0.915	-0.709
Patient #13 (θ=30°)	**The 30°'s B Matrix**	0.013	-0.164	0.026	0.067
		0.135	-0.042	-0.095	-0.033
		-1.026	-0.331	-1.109	-0.414
	The 45°'s B Matrix	0.160	-0.305	0.148	-0.062
		0.113	-0.020	-0.107	0.007
		-1.095	-0.286	-1.194	-0.404
	The 60°'s B Matrix	0.187	-0.326	0.176	-0.093
		0.171	-0.060	-0.062	-0.028
		-1.455	0.071	-1.502	-0.056
	The All12's B Matrix	0.098	-0.240	0.098	-0.009
		0.171	-0.073	-0.061	-0.044
		-1.100	-0.277	-1.187	-0.379

LIST OF REFERENCES

[1] Gregor ND, O'Connor DP, Edwards TB, Indications for reverse total shoulder arthroplasty in rotator cuff disease. Clin Orthop Relat Res. 2010; 468:1526–1533

[2] Boileau P, Sinnerton RJ, Chuinard C, Walch G. Arthroplasty of the shoulder. J Bone Joint Surg Br. 2006; 88(5):562-575

[3] Hatzidakis AM, Norris TR, Boileau P. Reverse shoulder arthroplasty indications, technique, and results. Tech Shoulder Elbow Surg. 2005; 6(3):135-149

[4] Leung B, Horodyski MB, Struk A, Wright T. Rotator cuff tear arthropathy: hemiarthroplasty or reverse total shoulder Arthroplasty? Open Meeting o the American Shoulder and Elbow Surgeons. San Diego, CA; Feb. 19, 2011

[5] Nam D, Kepler CK, Neviaser AS, Jones KJ, Wright TM, Craig EV, Warren RF. Reverse total shoulder arthroplasty: current concepts, results, and component wear analysis. J Bone Joint Surg Am. 2010; 92:23-35

[6] Wall B, Nove-Josserand L, O'Connor DP, Edwards TB, Walch G. Reverse total shoulder Arthroplasty: a review of results according to etiology. J Bone Joint Surg Am. 2007; 89:1476-1485

[7] Cheung E, Willis M, Walker M, Clark R, Frankle MA. Complications in reverse total shoulder arthroplasty. J Am Acad Orthop Surg. 2011; 19(7):439-49.

[8] Edwards TB, Williams MD, Labriola JE et al. Subscapularis insufficiency and the risk of shoulder dislocation after reverse shoulder arthroplasty. J Shoulder Elbow Surg. 2009 Mar 10.

[9] McFarland EG, Sanguanjit S, Tasaki A, Keyurapan E, Fishman EK, Fayad LM. The reverse shoulder prosthesis: a review of imaging features and complications. Skeletal Radiol. 2006; 35:488-496.

[10] Sanchez-Sotelo J. Reverse total shoulder arthroplasty. Clin Anat. 2008; 22(2): 172-82

[11] Tanino H, Higa M, Ito H, Sato T, Matsuno T, Banks SA. Intraoperative soft-tissue tension measurements during total hip Arthroplasty. In review, Clin Biomech 2010.

[12] Bergmann G, Graichen F, Bender A, Kaab M, Rohlmann A, Westerhoff P. In vivo glenohumeral contact forces—measurements in the first patient 7 months postoperatively. J. Biomech.2007; 40:2139–2149.

[13] Carlson KL. Human hip joint mechanics – an investigation into the effects of femoral head endoprosthetic replacement using in-vitro and in-vivo pressure data. PH.D. Thesis, Department of Mechanical Engineering, M.I.T., Boston, MA. 1993.

[14] Taylor SJG, Meswania JM, Rodríguez-Arias J, Calle R, Bayley IL, Blunn GW. An instrumented implant and calibration technique for measurement of glenohumeral joint forces In vivo. Proceedings of the 14th Conference of the European Society on Biomechanics, S-Hertogenbosch, The Netherlands. 2004.

[15] D'Lima DD, Patil S, Steklov N, Colwell, Jr. CM, In vitro and in vivo measurement of dynamic soft-tissue balancing during total knee arthroplasty with an instrumented tibial prosthesis. Trans. Annu. Meet. - Orthop. Res. Soc. 2004; 29.

[16] Bergmann G, Graichen F, Rohlmann A, Westerhoff P, Heinlein B, Bender A, Ehrig R. Design and calibration of load sensing orthopaedic implants. J. Biomech. Eng., 130 (2008), p. 021009

[17] Bergmann G. Ein Dreikomponenten-Kraftaufnehmer und Seine Anwendung für die Messung von Gelenkkräften am Tier. Ph.D. thesis, Technische Universität Berlin, Germany.1981.

[18] Bergmann G, Siraky J, Rohlmann A, and Kölbel R. 1982. Measurement of spatial forces by the ‘Matrix’-Method. Proceedings of the Ninth World Congress IMEKO, Berlin, Germany. 1982; pp. 395–404.

[19] Westerhoff P, Graichen F, Bender A, Rohlmann A, Bergmann G. An instrumented implant for in vivo measurement of contact forces and contact moments in the shoulder joint. Med Eng Phys. 2009; 31:207–213

BIOGRAPHICAL SKETCH

Chih-Chiang Chang was born in Taiwan in 1986. Chih-Chiang attended National Tsing Hua University where he received his B.Sc. in power mechanical engineering in 2008. He received his Master of Science degree in mechanical engineering from the University of Florida in May 2013. He majored in the study of orthopaedic biomechanics for his graduate study.